Reactions of Vibrationally Excited Ions. A Theoretical and Experimental Analysis of the Reaction $(C_4H_9^+)^* + NH_3 \rightarrow NH_4^+ + C_4H_8$

W. J. Chesnavich, T. Su, and M. T. Bowers*

Contribution from the Department of Chemistry, University of California, Santa Barbara, California 93106. *Received May 31, 1977*

Abstract: The rate constant of the reaction $t\text{-}C_4H_9^+ + NH_3 \rightarrow NH_4^+ + C_4H_8$ is shown to be strongly dependent on the electron energy used to generate the $t\text{-}C_4H_9^+$ ions from fragmentation of neo-C_5H_{12}. A statistical theory model is developed that conserves angular momentum. The theoretical model assumes a reaction mechanism of the form $t\text{-}C_4H_9^+ + NH_3 \rightleftarrows (C_4H_9NH_3^+) \rightarrow NH_4^+ + C_4H_8$. By comparison of theory to experiment, the electron energy dependence of the overall proton transfer reaction is shown to arise from competition between back reaction of the complex and reaction to produce $NH_4^+ + C_4H_8$. In order to fit the experimental data, it was necessary to assume a loose transition state for the formation of the NH_4^+, C_4H_8 products from $C_4H_9NH_3^+$. This transition state is not the intuitively most obvious one and a discussion is given of additional experimental and theoretical developments that would clarify the issue.

I. Introduction

The dependence of a reaction rate constant and reaction mechanism on energy is an important field of study in reaction kinetics and has received much attention in the past decade. In ion chemistry the earliest studies were carried out in single source mass spectrometers where the translational energy dependence of rate constants was measured as a function of repeller voltage.[1] Studies of translational energy dependence have since been refined by the introduction of tandem mass spectrometers, flowing afterglow/drift tubes, and molecular beam instruments.[2,3] The dependence of rates and mechanisms on internal energy in ion–molecule reactions has also become an active field, with the introduction and development of photoionization techniques primarily responsible. The dependence of rate constants and cross sections[4,5] on vibrational energy has been the primary focus of photoionization mass spectrometry but the study of the dependence of rate constants on electronic energy by photoionization[6,7] and other techniques[8] has begun in recent years.

Su and Bowers[9] have reported that the rate constant for the reaction

$$t\text{-}C_4H_9^+ + NH_3 \xrightarrow{k_2} NH_4^+ + i\text{-}C_4H_8 \qquad (1)$$

depends on the method of formation of $C_4H_9^+$ and on its internal energy. In this paper the results of a detailed experimental and theoretical study of this reaction are reported. Ion cyclotron resonance (ICR) spectroscopy and photoionization mass spectrometry are employed in the experiments. The $t\text{-}C_4H_9^+$ reactant ions are generated by the following reaction.

$$\text{neo-}C_5H_{12}^+ \rightarrow t\text{-}C_4H_9^+ + CH_3\cdot \qquad (2)$$

The $C_5H_{12}^+$ ions are prepared by electron impact ionization in the ICR spectrometer. The theoretical modeling uses statistical theory and relies on both orbiting and saddle point models for the various transition states involved in the reaction sequence. The internal energy distribution of the neo-$C_5H_{12}^+$ ions is estimated from an energy deposition function obtained from photoionization efficiency curves and an assumed linear electron impact ionization cross section law. A discussion of the approximations used in the theoretical calculations is provided.

II. Experimental Section

The ICR spectrometer used in these studies has been previously described.[10] The drift cell mode of operation was utilized to measure the rate constants. Pressures were measured using an MKS-Baratron capacitance manometer. Drift times were measured using the trapping plate ejection technique. The photoionization mass spectrometer used to obtain the ionization efficiency curves has been previously described.[11] All compounds used were the purest commercially available. No impurities were detected under the conditions of the experiments reported here.

Results. The results of the measurements of the rate constant of reaction 1 as a function of the nominal electron energy, V_0, for the ionization of neo-C_5H_{12} are plotted in Figure 1. The results are plotted as $k(V_0 - AP)/k(0)$ vs. $V_0 - AP$ where AP is the appearance potential for reaction 2. The value of $k(0)$, the thermal collision rate constant, is calculated from ADO theory.[12] At electron energies just slightly above the appearance potential of $t\text{-}C_4H_9^+$ the low signal to noise ratio makes measurements difficult and the uncertainty in the results increases. For this reason the value of the rate constant for reaction 1 measured by the flowing afterglow technique[13] is also reported in Figure 1. This value agrees quite well with the ADO prediction. Also included for comparison is the result obtained with $C_4H_9^+$ ions formed via the following reaction.[9]

$$C_4H_8^+ + i\text{-}C_4H_8 \rightarrow C_4H_9^+ + C_4H_7 \qquad (3)$$

The internal energy in the $C_4H_9^+$ ions generated by reaction 3 is not accurately known but is probably less than 0.5 eV.

The ionization efficiency curve for the appearance of $C_4H_9^+$ from neo-C_5H_{12} has been measured using photoionization mass spectrometry. The first derivative of this curve yields a good approximation of the energy deposition function associated with the $C_4H_9^+$ ion.[14] This derivative is given in Figure 2. The photoelectron spectrum of neo-C_5H_{12} in the energy range of interest is very similar in shape to the first derivative of the ionization efficiency curve as expected.[15] The data in Figure 2 will be used in the Theory section to approximate the energy distribution in the $C_4H_9^+$ ion formed by electron impact. It is assumed that all $C_4H_9^+$ ions formed from fragmentation of neo-C_5H_{12} are tertiary at all electron and photon energies used in the work reported here.

III. Theory

The theoretical treatment of the reaction sequence 2–1 is based on statistical theory. The orbiting transition state model[16,17] is used to determine the energy partitioning in reaction 2 and both orbiting and saddle point transition states are used for reaction 1. The effects of angular momentum are included. The results given in Figure 2, a threshold ionization law, and an appropriate ionizing electron energy distribution are used to estimate the internal energy distribution of the neo-$C_5H_{12}^+$ ions.

Consider first the fragmentation of $C_5H_{12}^+$. Rewriting reaction 2 to explicitly illustrate the energy partitioning gives

$$\text{neo-}C_5H_{12}^+ (E) \rightarrow t\text{-}C_4H_9^+ (E_1) + CH_3 (E_2) + E_{t0} \qquad (4)$$

0002-7863/78/1500-4362$01.00/0

In this reaction E is the internal energy of $C_5H_{12}^+$ above the appearance potential for fragmentation and E_{t0} is the relative translational energy of the fragments. The internal energies of the fragments, E_1 and E_2, are partitioned into vibration and rotation. Specifically,

$$E_1 = E_{v1} + B_1J_1^2 \tag{5a}$$

and

$$E_2 = E - E_1 - E_{t0} \tag{5b}$$

$$= E_{v2} + B_2J_2^2 \tag{5c}$$

where E_{v1} and E_{v2} are the vibrational energies of t-$C_4H_9^+$ and CH_3, respectively. B_1 and B_2 are their rotational constants and J_1 and J_2 are their rotational angular momenta. In writing eq 5 it has been assumed that t-$C_4H_9^+$ and CH_3 are spherical top rigid rotors with rotational constants given by $B = (ABC)^{1/3}$ and the rotational energy can be written in the classical form. The angular momentum partitioning in reaction 4 can be expressed as

$$\mathcal{J}_0 = \mathbf{J}_1 + \mathbf{J}_2 + \mathbf{L}_0 \tag{6}$$

where $\mathcal{J}_0$ is the rotational angular momentum of $C_5H_{12}^+$ and $\mathbf{L}_0$ is the orbital angular momentum of the fragments.

Since the fragmentation of neo-$C_5H_{12}^+$ and the proton transfer reaction occur in different center of mass systems, it is useful to consider first E_1 (lab), the laboratory kinetic energy of $C_4H_9^+$ after fragmentation. The contributions to E_1 (lab) arise from E_{th}, the thermal laboratory kinetic energy of $C_5H_{12}^+$, and from E_{t0}. After fragmentation the laboratory momentum of t-$C_4H_9^+$ is

$$\mathbf{p}_1 = \mathbf{p}_{10} + \mathbf{p}_{r1} \tag{7}$$

where $|p_{10}| = (2E_{th}m_1^2/M)^{1/2}$, $|p_{r1}| = (2\mu_{12}E_{t0})^{1/2}$, and μ_{12} is the reduced mass of $C_4H_9^+$ and CH_3. Using spherical polar coordinates to define the orientation of $\mathbf{p}_{r1}$ with respect to $\mathbf{p}_{10}$ gives

$$E_1(\text{lab}) = \frac{1}{2m_1}\mathbf{p}_1\cdot\mathbf{p}_1$$

$$= \frac{m_2}{M}E_{t0} + \frac{m_1}{M}E_{th} + \frac{2\sqrt{m_1m_2}}{M}\sqrt{E_{th}E_{t0}}\cos\theta \tag{8}$$

where m_1 and m_2 are the masses of t-$C_4H_9^+$ and CH_3, respectively, and M is the mass of $C_5H_{12}^+$. Equation 8 can now be averaged over θ weighed by $\sin\theta$ giving

$$\overline{E_1(\text{lab})} = \frac{m_1}{M}E_{th} + \frac{m_2}{M}E_{t0} \tag{9}$$

An estimate of the average E_{t0} predicted by the orbiting model can be obtained by noting that $C_5H_{12}^+$ has a thermal distribution of $\mathcal{J}_0$. In the limit $\mathcal{J}_0 \rightarrow 0$, Klots[16] has shown that

$$E_{t0} = \frac{2}{s+1}\frac{\int_0^E \rho_v(E_v)(E-E_v)^{s+1/2}\,dE_v}{\int_0^E \rho_v(E_v)(E-E_v)^{s-1/2}\,dE_v} \tag{10}$$

where $\rho_v(E_v)$ is the vibrational density of states of the fragments of reaction 4 at total vibrational energy E_v, and s is the total number of rotational degrees of freedom. Using the semiclassical limit for $\rho_v(E_v)$ gives

$$\overline{E_{t0}} = \frac{4}{581}(E + E_z) \tag{11}$$

where E_z is the total zero point vibrational energy of the fragments. For $E_z \sim 4$ eV and $E = 3.4$ eV (see Figure 2) eq 11 predicts $\overline{E_{t0}} \sim 0.052$ eV, which is truly an upper limit due to the semiclassical approximation used for $\rho_v(E_v)$. Therefore eq 9 and 11 suggest that the laboratory kinetic energy of t-$C_4H_9^+$ arises primarily from the thermal energy of $C_5H_{12}^+$.

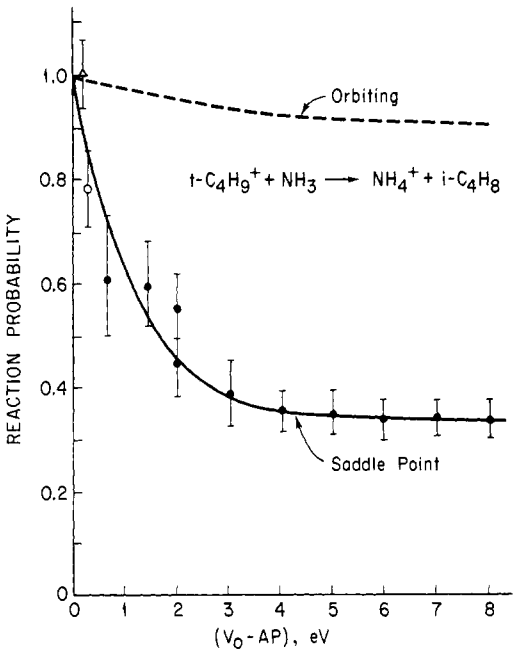

Figure 1. Dependence of the proton transfer reaction 1 on the nominal electron energy V_0. The results are plotted as $k_2(V_0 - \text{AP})/k_2(0)$ where AP is the appearance potential for the formation of t-$C_4H_9^+$, CH_3 from neo-C_5H_{12}. Experimental results: ●, ICR, this paper; ○, reaction 3 (ref 9); △, flowing afterglow (ref 13).

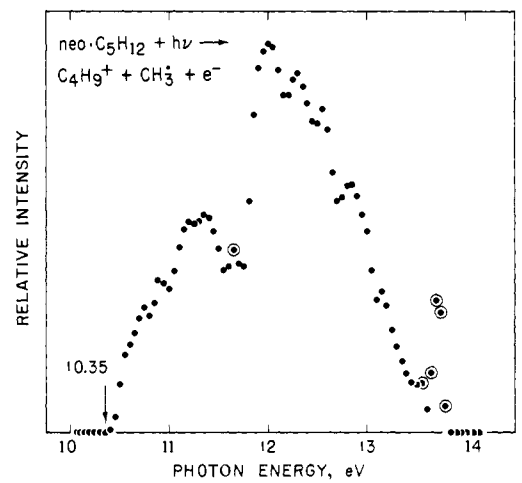

Figure 2. First derivative of the photoionization efficiency curve for formation of t-$C_4H_9^+$, CH_3 from neo-C_5H_{12}. The circled points are believed to be spurious.

When the assumption is made that E_{t0} in reaction 4 is carried off by the methyl radical the distribution of energies in the $C_4H_9^+$ fragment due to E becomes the vibrational-rotational distribution. According to the orbiting model this distribution can be written as

$$P(E,E_1,J_1) \propto 2\mathcal{J}_0\,\rho_{v1}(E_1 - B_1J_1^2)\,2J_1 \times \int W_{SA}(E - E_1, J')\,dJ' \tag{12}$$

where the limits on the integral are defined by the relation $\mathbf{J}' + \mathbf{J}_1 = \mathcal{J}_0$ and where $W_{SA}(E - E_1, J')$ is the J', J_z' conserved sum of vibrational-rotational-orbital states[17] with vibrational-rotational-translational energy equal to $E - E_1$ for an ion-neutral pair consisting of methyl radical and a structureless charged particle with mass equal to $C_4H_9^+$. The angular momentum J' is defined by $\mathbf{J}' = \mathbf{J}_2 + \mathbf{L}_0$ and J_z' is its projection

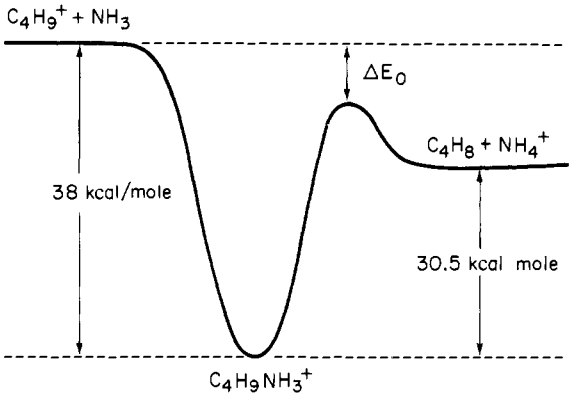

Figure 3. Schematic potential surface along hypothetical reaction coordinate for reaction 1.

on a space-fixed axis. In the limit $\mathcal{J}_0 \rightarrow 0$ the integration in eq 12 can be approximated as $2\mathcal{J}_0$ times the value of W_{SA} at $J' = J_1$, giving

$$P(E,E_1,J_1) \propto (2\mathcal{J}_0)^2 \rho_{v1}(E_1 - B_1J_1^2) \times 2J_1W_{SA}(E - E_1, J_1) \quad (13)$$

The normalization of eq 13 is obtained by integrating over J_1 within the range $0 \leq J_1 \leq J_1^*$ and over E_1 within the range $0 \leq E_1 \leq E$. The upper limit J_1^* is given by the lesser of $\sqrt{E_1/B_1}$ or that value of J_1 for which $W_{SA} = 0$. Since the rotational constant of CH_3 is large, W_{SA} becomes zero when J_1 is on the order of $[8\mu_{12}^2q^2\alpha_2(E - E_1)/\hbar^4]^{1/4}$ where α_2 is the polarizability of CH_3. Therefore

$$J_1^* \sim \text{lesser of } \{\sqrt{E_1/B_1};\ [8\mu_{12}^2q^2\alpha_2(E - E_1)/\hbar^4]^{1/4}\} \quad (14)$$

Although the average $\mathcal{J}_0$ of a thermal ensemble of neo-$C_5H_{12}^+$ ions is in the neighborhood of $\mathcal{J}_0 = 45$ at 300 K, eq 13 still provides a good estimate of $P(E,E_1,J_1)$ since the integration in eq 12 remains proportional to $2\mathcal{J}_0$ for $\mathcal{J}_0$ greater than zero.

Consider now the proton transfer reaction. The detailed mechanism of this reaction is assumed to be

$$t\text{-}C_4H_9^+ + NH_3 \underset{k_a}{\overset{k_c}{\rightleftharpoons}} [C_4H_9NH_3^+]^{\ddagger} \xrightarrow{k_b} NH_3^+ + i\text{-}C_4H_8 \quad (15)$$

where the $C_4H_9NH_3^+$ intermediate complex is assumed to undergo quasi-equilibrium before decomposing back to reactants or to products. Since the thermal overall forward rate constant for reaction 15 is in agreement with the ADO capture prediction (see Figure 1) it is assumed that the capture process is governed by an orbiting transition state. The charge-induced dipole long-range potential must be used for this transition state because the appropriate orbiting theory has not been developed for the charge-permanent dipole potential. Detailed balance requires that the same orbiting model used to calculate k_c must also be used to calculate k_a for the reverse decomposition reaction. Also since the t-$C_4H_9^+$ reagent ions are both rotationally and vibrationally excited, and since the rotational constants and vibrational frequencies of NH_3 are rather large, it is assumed that the internal energy of ammonia can be neglected.

With these assumptions in mind the overall forward rate constant for reaction 15, k_2, becomes

$$k_2(E_1,E_t,J_1) = \frac{1}{h\rho_t(E_t)2J_1} \int\int dL P(E_1 + E_t,\mathcal{J})\ 2\mathcal{J}\ d\mathcal{J} \quad (16)$$

where $\rho_t(E_t)$ is the relative translational density of states per unit volume for the t-$C_4H_9^+$, NH_3 reactant pair, L is the orbital momentum generated by the collision, and $\mathcal{J}$ is the total angular momentum of the system. The integrations in eq 16 are bounded by

$$\mathcal{J} = \mathbf{L} + \mathbf{J}_1 \quad (17a)$$

and

$$L \leq (8\mu^2q^2\alpha E_t/\hbar^4)^{1/4} \quad (17b)$$

where μ is the reduced mass of the t-$C_4H_9^+$, NH_3 pair, α is the polarizability of NH_3, and q is the charge on $C_4H_9^+$. The decomposition probability in eq 16 is given by

$$P(E_1 + E_t, \mathcal{J}) = [1 + k_a(E_1 + E_t, \mathcal{J})/k_b(E_1 + E_t + \Delta E_0, \mathcal{J})]^{-1} \quad (18)$$

where ΔE_0 is defined in Figure 3.

The unimolecular rate constants for orbiting (k_{orb}) and saddle point (k_{sp}) transition states at a given E and $\mathcal{J}$ can be written as[16,18]

$$k_{orb}(E,\mathcal{J}) = \mathcal{H}\frac{W_{ss}(E,\mathcal{J})}{h\rho(E_c,\mathcal{J})} \quad (19)$$

and

$$k_{sp}(E,\mathcal{J}) = \mathcal{H}\frac{W^{\ddagger}(E - B^{\ddagger}\mathcal{J}^2)2\mathcal{J}}{h\rho(E_c,\mathcal{J})} \quad (20)$$

In these equations $\mathcal{H}$ is the reaction path degeneracy and $\rho(E_c,\mathcal{J})$ is the density of states of the energized reagent at energy E_c. Also $W_{ss}(E,\mathcal{J})$ is the $\mathcal{J},\mathcal{J}_z$-conserved sum of states for two spherical top molecules at the orbiting transition state and $W^{\ddagger}(E - B^{\ddagger}\mathcal{J}^2)2\mathcal{J}$ is the $\mathcal{J},\mathcal{J}_z$-conserved sum of states at the saddle point transition state. Equation 20 assumes that the saddle point transition state can be approximated as a spherical top with rotational constant $B^{\ddagger}$ and internal degeneracy $2\mathcal{J}$. Equations 19 and 20 are functions of E, $\mathcal{J}$, and $\mathcal{J}_z$. In the calculations eq 19 was used for k_a and eq 19 and 20 were used for k_b.

In order to obtain the forward rate constant as a function of the $C_5H_{12}^+$ internal energy it is necessary to average eq 16 over the probability distribution given by eq 13. Before doing so it is worthwhile to note that the eq 16 is a function of E_1, J_{1z}, K_1, and J_1 where K_1 is the internal projection of J_1 on a molecular axis. Therefore $P(E,E_1,J_1)$ must include contributions due to internal and spatial symmetry. That these factors are included can be ascertained by noting that eq 12 includes a $2J_1$ factor for the internal projection of J_1 and a factor of $2\mathcal{J}_0$ due to spatial degeneracy. Therefore these equations can be combined in their current form giving

$$k_2(E,E_1) = \frac{1}{h\rho_t(E_t)} \int \frac{P(E,E_1,J_1)}{2J_1} \times dL\ dJ_1\ P(E_1 + E_t,\mathcal{J})\ 2\mathcal{J}\ d\mathcal{J}\ dE_1 \quad (21)$$

The boundaries on L are given by eq 17 and those on J_1 by eq 14. The integration over $\mathcal{J}$ goes from 0 to $L^* + J_1^*$ where L^* is given by eq 17b. The integration over E_1 is performed from $E_1 = 0$ to $E_1 = E$.

Equation 21 can now be convoluted over the thermal distribution of E_t modified by the fact that the laboratory kinetic energy of $C_4H_9^+$ is a factor of 57/72 smaller than the thermal laboratory kinetic energy of neo-$C_5H_{12}^+$. Calling this distribution $P_{mod}(E_t)$ gives

$$k_2(E) = \int P_{mod}(E_t)\ k_2(E,E_t)\ dE_t \quad (22)$$

It remains to determine the distribution of E as a function of the nominal ionizing energy V_0. Consider first electrons with kinetic energy V. The probability that these electrons create

neo-$C_5H_{12}^+$ ions with internal energy E above the appearance potential for fragmentation can be written as[19]

$$P(V,E) \propto Y(E)\,\sigma(V,E) \tag{23}$$

where $\sigma(V,E)$ is the cross section associated with the escape of product electrons with energy $V - AP - E$ and $Y(E)$ is the total transition probability for formation of neo-$C_5H_{12}^+$ ions with energy E from ground state neopentane neutrals. The exact form of $\sigma(V,E)$ is unknown. In the calculations reported here $\sigma(V,E)$ is assumed to be given by the following threshold law.[20,21]

$$\sigma(V,E) \propto (V - AP - E)^{r-1} \tag{24}$$

In eq 24 r is the number of electrons departing from the ionization region. For electron impact ionization $r = 2$. The photoionization results reported in Figure 2 are used for the transition probabilities. This choice assumes that $Y(E)$ is independent of the method of ionization.[21]

The normalization of eq 23 is governed by the fact that the total probability that the t-$C_4H_9^+$, CH_3 fragments have energy between zero and the lesser of $V - AP$ or the upper limit of Figure 2 is unity.

Equation 23 must also be convoluted with $P(V_0,V)$, the probability that a nominal ionizing energy V_0 produces electrons of energy V. This probability depends on the thermal spread of electron energies and, for ICR, on the modification of the thermal spread by the ICR trapping voltage.[22] However, owing to the form of the threshold law used in the calculations the spread in electron energies is important only at nominal electron energies in the immediate vicinity of the appearance potential. Since this region is also the region in which the experimental results are least accurate the calculations were simplified by choosing a thermal distribution (T = 1900 K) for $P(V,V_0)$. The final result is, therefore,

$$k_2(V_0) = \int\int dV\,dE\,P(V_0,V)\,P(V,E)\,k_2(E) \tag{25}$$

IV. Results and Discussion

A variety of calculations were performed. Both orbiting (eq 19) and saddle point (eq 20) transition states were used for the proton transfer rate constant k_b in reaction 15. Since the overall reaction rate constant, k_2, proceeds at the capture limit at energies near the appearance potential for formation of t-$C_4H_9^+$ (as shown by the flowing afterglow result in Figure 1), only an orbiting transition state was used for the collision of t-$C_4H_9^+$ and NH_3 to form the $C_4H_9NH_3^+$ intermediates and for the reverse dissociation reaction (k_c and k_a, respectively, in reaction 15). The calculation of $k_2(E)$ using eq 22 was found to be only mildly sensitive to E_t in its range of most probable values. A number of effects contribute to this result including the fact that the decomposition probability eq 18 is given by a ratio, the fact that there is a broad distribution in E_1, and the fact that the distribution of J_1 favors reasonably large values of J_1. Also, $k_2(V_0)$ was rather insensitive to the exact form of $P(V_0,V)$ used in eq 25. The sensitivity was strongest near V_0 = AP, and, as expected, became nonexistent near V_0 = 4 eV.

The data used in the calculations that agreed best with experiment are given in Table I. The results of these calculations are plotted in Figure 1. A word should be said at this point about reaction path degeneracies ($\mathcal{H}$ in eq 19 and 20). For an orbiting transition state $\mathcal{H}$ is given by the ratio of the product of symmetry numbers of the products to that of the reactant as can be verified by direct count.[23] For saddle point transition states a direct count must be used.[24] Only ratios of $\mathcal{H}$'s enter into the decomposition probability eq 18. When orbiting transition states were used for both decomposition channels $\mathcal{H}_a/\mathcal{H}_b = 4/9$. When a saddle point transition state was used for the proton transfer channel $\mathcal{H}_a/\mathcal{H}_b = 1/2$. These numbers include the effects of conversion of internal free rotation of the $C_4H_9NH_3^+$ complex to overall rotations of the products.

Table I. Data Used in the Statistical Theory Calculations

Species	Rotational constant, cm^{-1} [a]	$\alpha \times 10^{24}$, cm^3	$\Delta H_f°$, 298, kcal/mol[b]
$C_4H_9^+$	0.250		169[c]
CH_3	7.64	2.2	
NH_3	8.45	2.26	−11.0[d]
C_4H_8	0.236	7.52	−4.04[d]
NH_4^+	5.24		154.5[e]

Vibrational Frequencies, cm^{-1}

$C_4H_9^+$	CH_3	NH_3	C_4H_8	NH_4^+	Proton transfer transition state
2900 (9)	3100 (2)	3400 (8)	300 (8)	3400 (3)	3400 (3)
1500 (9)	3000 (1)	1600 (2)	1700 (1)	3300 (1)	2900 (8)
1100 (8)	1400 (2)	950 (1)	1500 (6)	1600 (2)	1500 (11)
800 (1)	800 (1)		1100 (8)	1300 (4)	1100 (9)
500 (2)			800 (2)		800 (2)
250 (4)[f]			500 (1)		750 (1)
			250 (4)[f]		550 (1)
					500 (1)
					250 (4)
					150 (2)
					6.5 (2)[g]

[a] The rotational constant for the saddle point transition state for the proton transfer reaction was taken to be 0.10 cm^{-1}. [b] The appearance potential for reaction 2 was taken to be 10.35 eV. [c] F. P. Lossing and G. P. Semeluk, *Can. J. Chem.*, **48**, 955 (1970); see also W. Tsang, *J. Phys. Chem.*, **76**, 143 (1972). [d] J. L. Franklin, J. G. Dillard, H. M. Rosenstock, J. T. Heron, K. Draxl, and F. H. Field, NSRDS-NBS 26 (1969). [e] R. Yamdagni and P. Kebarle, *J. Am. Chem. Soc.*, **98**, 1920 (1976). [f] When orbiting transition states were used for both channels the three torsions of $C_4H_9^+$ and the two torsions of C_4H_8 at 250 cm^{-1} were converted to free rotors with B = 6.5 cm^{-1}. The reasons for doing this are explained in the text. [g] Free rotor.

When an orbiting transition state was used for the proton transfer channel (with ΔE_0 equal to the reaction exoergicity) the calculated curve did not exhibit the falloff with respect to V_0 observed in the experiments (see Figure 1). This type of behavior has been observed in other systems.[25] It is due primarily to the fact that there are the same number of orbital and overall rotational degrees of freedom in the transition state for each decomposition channel and hence the density of states in the more exothermic channel far exceeds that in the less exothermic channel until the system energy far exceeds ΔE_0.

It should be noted that the results reported here for an orbiting transition state in the proton transfer channel used $C_4H_9^+$ and C_4H_8 structures altered in a manner to emphasize most strongly any falloff in $k_2(V_0)$ with respect to V_0. This was accomplished by changing all CH_3 torsions in these molecules to free rotations. This choice provides the t-$C_4H_9^+$, NH_3 channel with an extra internal rotational degree of freedom with respect to the C_4H_8, NH_4^+ channel. The choice is not physically reasonable and is used to emphasize the failure of the orbiting model for this reaction channel. When the calculations were performed without including free rotations in t-$C_4H_9^+$ and i-C_4H_8 the falloff of $k_2(V_0)$ with respect to V_0 was even less than the result reported in Figure 1.

When a saddle point transition state was used for the proton transfer channel it was possible to obtain agreement between experiment and theory by choosing ΔE_0 equal to the reaction exoergicity and by choosing a very loose transition state structure. The transition state parameters used in the calculations reported here were obtained by estimating the vibra-

tional frequencies of $C_4H_9NH_3^+$ by comparison to neo-C_5H_{12}, choosing a CH stretch as the reaction coordinate, and decreasing the six vibrational frequencies that pass to rotations and translations of the i-C_4H_8, NH_4^+ products (assumed to be 1500 (1), 1100 (1), 500 (2), 250 (2) cm^{-1}) by one-half. Also the torsional motions associated with the two methyl groups of the transition state structure were changed to free rotations and the overall rotational constant was chosen to be $B^{\ddagger} = 0.10$ cm^{-1}. This choice of transition state is not unreasonable for some simple bond cleavages. Intuition suggests, however, that the proton transfer reaction may well proceed through a tighter four-center transition state than that chosen for the calculations.

There are a number of possible reasons why the theoretical model used to reproduce the experimental results does not correspond to the physically most reasonable model. First, the energy distribution of the neo-$C_5H_{12}^+$ ions is not really well known. The agreement between the results of Figure 2 and the photoelectron spectrum of neo-C_5H_{12} suggests that the transition probabilities ($Y(E)$ in eq 23) are accurately given by Figure 2, at least for photoionization. However, the use of the linear ionization cross section law for electron impact ionization is open to question. This uncertainty could be removed to a large extent by performing the experiments using photoionization.[5,6]

Second, the energy partitioning in the fragmentation of the $C_5H_{12}^+$ ions is not known. Recent monoenergetic experiments[26] have enabled the orbiting model to be tested for the prediction of translational energy release. The results for reagents with a thermal distribution of δ have been mixed.[18,26] It appears that for fragmentation occurring with rate constants on the order of 10^6 s^{-1} the orbiting model gives reasonable agreement with experiment for reaction with no reverse activation energy.[18] However, as the fragmentation rate increases experiment and theory may begin to diverge.[26] No experiments have been reported for vibrational and/or rotational energy disposal in ionic systems. In order to overcome this uncertainty it would be desirable to obtain data on the absolute magnitude of k_2 as a function of the internal energy of $C_4H_9^+$ ions.

Third, the proton transfer reaction may occur in part through a direct process. This possibility can be tested most readily by studying the angular distribution of the products in beam experiments. The resulting product translational energy distributions would also be informative since four-center reaction mechanisms are usually expected to have a reverse activation energy.[27]

Fourth, the orbiting model may not adequately describe the energy dependence of the decomposition of the $C_4H_9NH_3^+$ complex back into the t-$C_4H_9^+$, NH_3 reactant channel. The orbiting model generally fails to describe the energy dependence of unimolecular rate constants for reagents with a thermal distribution of angular momenta.[16,18] Also, in the cases reported so far it does not provide a good description of competition between various product channels in bimolecular reactions.[25] If this is the case, however, then the theoretical question arises as to how one can construct a transition state which reduces to the orbiting model at low energies and to a more restrictive saddle point model at high energies.

In summary, the statistical theory model described here can adequately mimic the behavior of $k_2(V_0)$ as V_0 varies by choosing a loose transition state for the proton transfer exit channel of the $C_4H_9NH_3^+$ collision complex. A loose transition state for this reaction is not intuitively the most reasonable transition state but cannot be ruled out. Crucial experiments on the kinetic energy distribution of the NH_4^+, C_4H_8 fragments need to be done to establish whether or not a barrier exists in the reverse reaction. The existence of such a barrier would be strong evidence that a tight transition state is appropriate for the proton transfer exit channel and that the current theoretical model would have to be modified.

Acknowledgments. The authors gratefully acknowledge the support of the National Science Foundation under Grants CHE74-18397 and CHE77-15449 and the donors of the Petroleum Research Fund, administered by the American Chemical Society, for partial support of this research. The assistance of Dr. Ashley Williams in obtaining the photoionization efficiency curve of $C_4H_9^+$ from neo-C_5H_{12} is also gratefully acknowledged. The photoionization mass spectrometer used for this determination was constructed with the aid of a grant from the President's Fund, California Institute of Technology.

References and Notes

(1) For a collection of some of the earlier work see "Ion Molecule Reactions in the Gas Phase", *Adv. Chem. Ser.*, **No. 58** (1966).
(2) A more recent review of techniques in ion chemistry is found in J. L. Franklin, Ed., "Ion-Molecule Reaction", Plenum Press, New York, N.Y., 1972.
(3) See also P. Ausloos, Ed., "Interactions between Ions and Molecules", Plenum Press, New York, N.Y., 1975.
(4) See the chapter by W. A. Chupka in ref 2 for a discussion.
(5) For a recent paper, see P. R. Le Brenton, A. D. Williamson, J. L. Beauchamp, and W. T. Huntress, *J. Chem. Phys.*, **62**, 1623 (1975).
(6) See chapter by W. A. Chupka in ref 3.
(7) For other examples see J. M. Ajello, W. T. Huntress, A. L. Lane, P. R. Le Breton, and A. D. Williamson, *J. Chem. Phys.*, **60**, 1211 (1974); J. M. Ajello, K. D. Pang, and K. M. Monalian, *ibid.*, **61**, 3152 (1974).
(8) For some leading references on electron impact work see L. Freedman and B. G. Reuben, *Adv. Chem. Phys.*, **19**, 33 (1971); M. T. Bowers, M. Chau, and P. R. Kemper, *J. Chem. Phys.*, **63**, 3656 (1975).
(9) T. Su and M. T. Bowers, *J. Am. Chem. Soc.*, **95**, 7611 (1973).
(10) V. G. Anicich and M. T. Bowers, *Int. J. Mass Spectrom. Ion Phys.*, **11**, 89 (1973); V. G. Anicich, Ph.D. Thesis, University of California, Santa Barbara, 1973.
(11) P. R. Le Breton, A. D. Williamson, J. L. Beauchamp, and W. T. Huntress, *J. Chem. Phys.*, **62**, 1623 (1975).
(12) T. Su and M. T. Bowers, *Int. J. Mass Spectrom. Ion Phys.*, **12**, 347 (1973); L. Bass, T. Su, W. J. Chesnavich, and M. T. Bowers, *Chem. Phys. Lett.*, **34**, 119 (1975).
(13) R. S. Hemsworth, J. D. Payzant, J. I. Schiff, and D. K. Bolhme, *Chem. Phys. Lett.*, **26**, 417 (1974).
(14) W. A. Chupka and J. Berkowitz, *J. Chem. Phys.*, **47**, 2921 (1967).
(15) M. T. Bowers, unpublished data.
(16) K. C. Klots, *Z. Naturforsch. A*, **27**, 553 (1971).
(17) W. J. Chesnavich and M. T. Bowers, *J. Chem. Phys.*, **66**, 2306 (1977).
(18) W. J. Chesnavich and M. T. Bowers, *J. Am. Chem. Soc.*, **99**, 1705 (1977).
(19) (a) See, for example, H. M. Rosenstock and M. Kraus, "Mass Spectrometry of Organic Ions", F. W. McLafferty, Ed., Academic Press, New York, N.Y., 1963, Chapter 1. (b) See also the discussion by M. Vestal in "Fundamental Processes in Radiation Chemistry", P. J. Ausloos, Ed., Interscience, New York, N.Y., 1968.
(20) A. Wannier, *Phys. Rev.*, **90**, 817 (1953); **100**, 1180 (1956); S. Geltman, *ibid.*, **102**, 171 (1956); I. Kang and W. D. Foland, *ibid.*, **164**, 122 (1967). See also the reviews by M. R. H. Rudge, *Rev. Mod. Phys.*, **40**, 564 (1968); C. E. Klots in ref 19b.
(21) See, for example, discussions in J. D. Morrison, *J. Chem. Phys.*, **21**, 1767 (1953); W. A. Chupka and M. Korminsky, *ibid.*, **35**, 1991 (1961); W. A. Chupka and J. Berkowitz, *ibid.*, **47**, 2921 (1967); G. G. Meisels, J. Y. Park, and B. G. Geisner, *J. Am. Chem. Soc.*, **92**, 254 (1970); S. E. Scheppele, R. K. Mitchum, K. F. Kinneberg, G. G. Meisels, and R. H. Emmel, *ibid.*, **95**, 5105 (1973).
(22) W. J. Chesnavich, T. Su, and M. Bowers, *J. Chem. Phys.*, **65**, 990 (1976).
(23) C. E. Klots, *J. Phys. Chem.*, **75**, 1526 (1971).
(24) W. Forst, "Theory of Unimolecular Reactions", Academic Press, New York, N.Y., 1973.
(25) W. J. Chesnavich and M. T. Bowers, *J. Am. Chem. Soc.*, **98**, 8301 (1976); *Chem. Phys. Lett.*, **52**, 179 (1977).
(26) C. E. Klots, D. Mintz, and T. Baer, *J. Chem. Phys.*, **66**, 5100 (1977), and references cited therein.
(27) See, for example, the experimental confirmation by W. T. Huntress, D. Sen Sharma, K. R. Jennings, and M. T. Bowers, *Int. J. Mass Spectrom. Ion Phys.*, **24**, 25 (1977), of the reverse activation energy predicted by M. T. Bowers, W. J. Chesnavich, and W. T. Huntress, *ibid.*, **12**, 357 (1973).